

# Significant X-ray Line Emission in the 5-6 keV band of NGC 4051

T.J.Turner

*Department of Physics, University of Maryland Baltimore County, Baltimore, MD 21250 and Astrophysics Science Division, NASA/GSFC, Greenbelt, MD 20771, U.S.A*

L.Miller

*Dept. of Physics, University of Oxford, Denys Wilkinson Building, Keble Road, Oxford OX1 3RH, U.K.*

J.N.Reeves, A. Lobban

*Astrophysics Group, School of Physical and Geographical Sciences, Keele University, Keele, Staffordshire ST5 5BG, U.K*

V.Braitto

*Department of Physics and Astronomy, University of Leicester, University Road, Leicester LE1 7RH, UK*

S.B.Kraemer

*Institute for Astrophysics and Computational Sciences, Department of Physics, The Catholic University of America, Washington, DC 20064; and Astrophysics Science Division, NASA Goddard Space Flight Center, Greenbelt, MD 20771*

and

D.M.Crenshaw

*Department of Physics and Astronomy, Georgia State University, Astronomy Offices, One Park Place South SE, Suite 700, Atlanta, GA 30303, USA*

## ABSTRACT

A *Suzaku* X-ray observation of NGC 4051 taken during 2005 Nov reveals line emission at 5.44 keV in the rest-frame of the galaxy which does not have an obvious origin in known rest-frame atomic transitions. The improvement to the fit statistic when this line is accounted for establishes its reality at  $> 99.9\%$  confidence: we have also verified that the line is detected in the three XIS units independently. Comparison between the data and Monte Carlo simulations shows that the probability of the line being a statistical fluctuation is  $p < 3.3 \times 10^{-4}$ . Consideration of three independent line detections in *Suzaku* data taken at different epochs yields a probability  $p < 3 \times 10^{-11}$  and thus conclusively demonstrates that it cannot be a statistical fluctuation in the data. The new line and a strong component of Fe K $\alpha$  emission from neutral material are prominent when the source flux is low, during 2005. Spectra from 2008 show evidence for a line consistent with having the same flux and energy as that observed during 2005, but inconsistent with having a constant equivalent width against the observed continuum. The stability of the line flux and energy suggests that it may not arise in transient hotspots, as has been suggested for similar lines in other sources, but could arise from a special location in the reprocessor, such as the inner edge of the accretion disk. Alternatively, the line energy may be explained by spallation of Fe into Cr, as discussed in a companion paper.

## 1. Introduction

New X-ray data from high-throughput missions such as *XMM-Newton* and *Suzaku*, along with the high spectral resolution afforded by the *Chandra* High Energy Transmission Grating (HETG) has led to the discovery of several important spectral signatures in Active Galactic Nuclei (AGN) that were not detectable using previous missions.

A joint *XMM-Newton/Chandra* observation of NGC 3516 (Turner et al. 2002) revealed the first detection of narrow line emission at 5.6 and 6.2 keV (the latter was able to be resolved from the strong Fe  $K\alpha$  line owing to the relatively high spectral resolution afforded by the HEG grating). While the line energies matched those expected for ionized species of Cr and Mn, the line strengths exceeded what might be expected from illumination of material with cosmic abundance ratios. One explanation considered was enhancement of Cr and Mn abundances from spallation of Fe. However, this was initially disfavored as the line ratios did not agree well with those predicted by Skibo (1997) for spallation of disk gas (Turner et al. 2002). The alternative possibility, of Doppler-shifted components of Fe emission, led to a suggestion of emitting hotspots on the accretion disk surface - with an expectation of observable shifts in line flux and energy as the hotspot traverses its orbit. Further examples of the phenomenon, dubbed ‘transient Fe lines’, soon came from observations of other AGN, with many lines reported in the 5-6 keV regime (e.g. Yaqoob et al. 2003; Turner et al. 2004).

In this paper we report the highly significant detection of an emission line at 5.44 keV in the rest-frame of the nearby narrow line Seyfert 1 type AGN NGC 4051. The systemic redshift of the host galaxy is  $z = 0.0023$  that yields a distance 9.3 Mpc for  $H_0 = 74 \text{ km s}^{-1} \text{ Mpc}^{-1}$  assuming the redshift to arise from the Hubble flow. However, for such nearby galaxies a more reliable estimation of distance can be obtained from use of the Tully-Fisher relation, giving a distance of 15.2 Mpc (Russell 2004) in this case, which we adopt in this paper.

NGC 4051 was observed by *Suzaku* in 2005 and 2008. The 2005 observations have previously been described and analyzed by Terashima et al. (2009), who showed that the X-ray source was highly vari-

able on short timescales, and that a spectral model including variable partial-covering absorption was required to fit the data. Here we make a joint analysis of the 2005 observation together with the new 2008 data in which we concentrate specifically on the detection of the narrow emission line and its variability. We then discuss the possible origin of the line in the context of several popular models.

## 2. Observations

The *Suzaku* X-ray Imaging Spectrometer (XIS Koyama et al. 2007) instrument comprises four X-ray telescopes (Mitsuda et al. 2007) each with a CCD in the focal plane. XIS CCDs 0,2,3 are configured to be front-illuminated (FI) and provide useful data over  $\sim 0.6 - 10.0$  keV with energy resolution FWHM  $\sim 150$  eV at 6 keV. XIS 1 is a back-illuminated CCD and has an enhanced soft-band response (down to 0.2 keV) but lower area at 6 keV than the FI CCDs as well as a larger background level at high energies, consequently this detector was not used in our analysis. *Suzaku* also carries a non-imaging, collimated Hard X-ray Detector (HXD Takahashi et al. 2007) whose PIN instrument provides useful data over 15-70 keV for bright AGN.

Our analysis used all available *Suzaku* observations of NGC 4051 comprising data from 2005 Nov 10-13 (observation identifier 700004010) and 2008 Nov 6-12 (703023010) and 23-25 (703023020) as summarized in Table 1. The data were reduced using v6.4.1 of HEASOFT and screened to exclude: i) periods during and within 500 seconds of the South Atlantic Anomaly (SAA), ii) with an Earth elevation angle less than  $10^\circ$  and iii) with cut-off rigidity  $> 6$  GeV. The source was observed at the nominal center position for the XIS during 2008 and at the nominal center position for the HXD during 2005. The FI CCDs were in  $3 \times 3$  and  $5 \times 5$  edit-modes, with normal clocking mode. For the XIS we selected events with grades 0,2,3,4, and 6 and removed hot and flickering pixels using the SISCLEAN script. The spaced-row charge injection (SCI) was used. The XIS products were extracted from circular regions of  $2.9'$  radius with background spectra from a region of the same size, offset from the source (avoiding the calibration sources at the edges of the chips). The response

and ancillary response files were created using XIS-RMFGEN v2007 MAY and XISSIMARFGEN v2008 MAR.

NGC 4051 is too faint to be detected in the HXD GSO instrument, but was detectable in the PIN. For the analysis we used the model “D” background (Fukazawa et al. 2009). As the PIN background rate is strongly variable around the orbit, we first selected source data to discard events within 500s of an SAA passage, we also rejected events with day/night elevation angles  $> 5^\circ$ . The time filter resulting from the screening was then applied to the background events model file to give PIN model-background data for the same time intervals covered by the on-source data. As the background events file was generated using ten times the actual background count rate, an adjustment to the background spectrum was applied to account for this factor. HXDDTCOR v2007 MAY was run to apply the deadtime correction to the source spectrum. To take into account the cosmic X-ray background (Boltdt & Leiter 1987; Gruber et al. 1999) XSPEC v 11.3.2ag was used to generate a spectrum from a CXB model (Gruber et al. 1999) normalized to the  $34' \times 34'$  *Suzaku* PIN field of view, and combined with the PIN instrument background file to create a total background file. The mean exposure times for XIS are given in Table 1. The exposure times for the PIN were 112, 204 and 59 ks for 2005 Nov 10, 2008 Nov 6 and 2008 Nov 23, respectively.

Spectral fits used data from XIS 0, 2 and 3, for the 2005 data. As use of XIS2 was discontinued after a charge leak was discovered in Nov 2006, the 2008 analysis used only XIS 0 and 3. In this paper, XIS data were fit over 3.0 – 10 keV. PIN data were fit simultaneously with the XIS, in the range 15-50 keV. In the spectral analysis, the PIN model flux was increased by a factor 1.16 for 2008 data and 1.18 for 2005 data, which are the appropriate adjustments for the instrument cross-calibration at those epochs of the observation. XIS data were binned at the HWHM instrumental resolution while PIN data were binned to be a minimum of  $5\sigma$  above the background level for the spectral fitting.

### 3. Spectral Fitting

The mean *Suzaku* count rate over 0.5-10 keV during the low state of 2005 was 0.45 XIS counts $s^{-1}$  per FI XIS and 0.04 PIN counts $s^{-1}$ . During the high-state of 2008 Nov 6 it was 2.06 XIS counts $s^{-1}$  per FI XIS and 0.07 PIN counts $s^{-1}$  (Table 1). The count rates recorded correspond to an observed 2-10 keV flux range  $0.87 - 2.42 \times 10^{-11}$  erg cm $^{-2}$ s $^{-1}$  and a 10-50 keV flux range  $2.44 - 3.63 \times 10^{-11}$  erg cm $^{-2}$ s $^{-1}$ . The 2005 data represent a historically low state, as noted by Terashima et al. (2009) and during 2008 the source was close to the historical average flux level. The 2008 Nov 6 *Suzaku* observation was accompanied by a contemporaneous HETG exposure that reveals a wealth of emission and absorption features from several zones of ionized gas. The HETG analysis will be described in detail in another paper (Lobban et al. 2010).

#### 3.1. Fitting the PCA Offset Component

To assist in modeling the full-band *Suzaku* data, we first performed a decomposition of the events from all three *Suzaku* observations using Principal Components Analysis using the SVD method and code of Miller et al. (2007). A full description of the PCA decomposition of these data is reported by Miller et al. (2009). In summary, PCA is a mathematical decomposition of the data into orthogonal ‘eigenvectors’. The dominant variations are ascribed to eigenvectors of the lowest orders. In the case of NGC 4051 the data were found to be well-described by a steady “offset” component having a hard spectrum (Figure 1 and see Miller et al. 2009) while the first order variable component, eigenvector 1, is consistent with an absorbed power-law of constant slope whose variations in intensity dominate the spectral variability of the source (consistent with the analysis of Terashima et al. 2009). The physical origin of the offset component is of great interest. The low-state spectrum of NGC 4051 is composed of this component plus some contribution by eigenvector 1. Fitting the lowest flux subset of the 2005 data, Terashima et al. 2009 found the hard component to be best described using a partially-covered reflection component. Our analysis of the PCA offset component provides another way to probe the lowest flux levels of the

source and, while we find an acceptable fit using a combination of reflection (modeled using PEXRAV) plus a contribution from the powerlaw continuum ( $\Gamma = 2.3$ , fixed from fitting eigenvector 1), both emission components require absorption by a complex of ionized gas. Fortunately the multiple layers of ionized gas can be well constrained using HETG and LETG data (Collinge et al. 2001; Steenbrugge et al. 2009; Lobban et al. 2010), reducing the degeneracy of the *Suzaku* fit. In addition to these components, Fe K $\alpha$  line emission is evident in the offset spectrum at a fitted energy  $E = 6.398 \pm 0.023$  keV having a width  $\sigma = 0.045^{+0.037}_{-0.045}$  keV and flux  $n = 1.90 \pm 0.26 \times 10^{-5}$  photons  $\text{cm}^{-2} \text{s}^{-1}$ . (Throughout this paper, errors are quoted at 90% confidence for the appropriate number of interesting parameters in the fit.) The resulting fit statistic was  $\chi^2 = 130/153$  *d.o.f.*

Intriguingly, the normalization of the reflection continuum is extremely high relative to that of the primary continuum. The inconsistency of reflection and continuum strengths may indicate that the partial-covering absorption comprises a larger part of this component than currently modeled. The relatively high flux of the hard component was also noted by Terashima et al. (2009) based upon fitting the 2005 data, and is fully explored by Lobban et al. (2010).

In addition to the prominent narrow Fe K line, a strong excess of line emission is evident in the PCA offset spectrum, at 5.44 keV (Figure 1). No significant residuals appear in eigenvector 1 at that energy (Miller et al. 2009). The new line is thus consistent with having an origin associated with the hard offset component and neutral component of Fe K $\alpha$  emission.

### 3.2. Fitting the 2008 Contemporaneous Chandra and Suzaku data

As the 2008 Nov 6 epoch provides contemporaneous HEG data for the *Suzaku* observation, we fit those spectra together over 3-8 keV, combining the superior energy-resolution of HEG and the good statistical quality of the FI XIS units (0,3) to obtain the best possible constraints on the width and energy of the neutral component of Fe K $\alpha$ . A joint fit to those data using a simple powerlaw plus single Gaussian line showed residual excesses in the 5 - 6 keV band in *Suzaku* XIS data (Figure 2).

We refit, adding to the model a single component of absorption, a Gaussian representation of the K $\beta$  line fixed at a rest-energy of 7.05 keV with a flux linked to be 13.5% of the K $\alpha$  component (e.g. Leahy & Creighton 1993; Palmeri et al. 2003), a narrow absorption line detected at an observed energy of 7.1 keV (as discovered by Pounds et al. 2004 and confirmed by Terashima et al. 2009) plus a component to model the narrow line emission evident at 6.62 keV in HEG data (Lobban et al. 2010). The fit yielded a line energy  $E = 6.410 \pm 0.015$  keV, width  $\sigma = 50^{+26}_{-33}$  eV and normalization  $n = 1.90 \pm 0.395 \times 10^{-5}$  photons  $\text{cm}^{-2} \text{s}^{-1}$ . The equivalent width for the Fe K $\alpha$  line component is 95 eV against the total continuum level observed during 2008. The constraint on the width of the Fe K $\alpha$  line is equivalent to a FWHM velocity-broadening of  $5540^{+2846}_{-3664}$   $\text{km s}^{-1}$  (90 percent confidence interval). Assuming the true line centroid energy to be 6.40 keV, the 90% confidence constraint on energy from the combined HEG/XIS data limits the bulk velocity of this emitter to  $250 \gtrsim v \gtrsim -1200$   $\text{km s}^{-1}$  where negative velocity denotes outflow.

As the PCA decomposition indicates the presence of a weak broad component of Fe K $\alpha$  on eigenvector 1 (Miller et al. 2009), we tried adding a second component of Fe K $\alpha$  emission to the model, with the energies of both line components linked. This addition improved the fit-statistic by  $\Delta\chi^2 = 5$ , giving the same line energy as for the single component model, with  $\sigma_1 = 1^{+23}_{-1}$  eV and normalization  $n_1 = 1.12 \pm 0.32 \times 10^{-5}$  photons  $\text{cm}^{-2} \text{s}^{-1}$  (EW= 41 eV),  $\sigma_2 = 145^{+70}_{-52}$  eV and normalization  $n_2 = 1.07 \pm 0.45 \times 10^{-5}$  photons  $\text{cm}^{-2} \text{s}^{-1}$  (EW= 43 eV). Although the two-component parameterization of Fe K $\alpha$  offers only a marginal improvement to the fit, it is of interest with regard to consistency with the PCA decomposition, which indicates the weak broad component of Fe K $\alpha$  emission to be present on eigenvector 1.

In subsequent fits we fix the Fe K $\alpha$  model line width at  $\sigma = 50$  eV obtained from the simple fit, while bearing in mind the possible more complex solution for the line profile. As the PCA is consistent with a common origin for Fe K $\alpha$  emission and the line at 5.44 keV, and as the widths of the two lines are consistent (and as there is no other useful constraint available for the indeterminate line

width) hereafter we fixed both to  $\sigma = 50$  eV in spectral fitting.

### 3.3. Fitting the 2005 Suzaku data

To assess the significance of the line at 5.44 keV we returned to direct fitting of the 2005 data, where the source was observed to be at a low flux and where PCA indicates that the line would have the highest equivalent width. We fit the summed 2005 data from the FI XIS units 0, 2 and 3 using an absorbed continuum model, applying it to the 3-10 keV band for the purpose of examining the data for features of interest. A Gaussian line was included in the fit, to account for the Fe K $\alpha$  emission, fixed at the energy and width found using HEG/XIS. As evident in Figure 3 the mean spectrum from 2005 data shows an excess of counts at 5.44 keV with additional structure evident around 6 keV. We performed a more complex fit to properly assess the line strengths and significance. We added to the model a Gaussian representation of the Fe K $\beta$  line fixed at a rest-energy of 7.05 keV with a flux linked to be 13.5% of the K $\alpha$  component. The model also included the narrow absorption line detected at an observed energy of 7.1 keV as discovered by Pounds et al. (2004) and confirmed by Terashima et al. (2009), plus a component to model the narrow line emission evident at 6.62 keV (Lobban et al. 2010). The fit yielded  $\chi^2 = 176/101$  *dof* and the strongest unmodeled feature remains evident as an excess of counts at 5.44 keV.

Addition of a Gaussian line ( $\sigma = 50$  eV) reduced the fit-statistic by  $\Delta\chi^2 = 32$ , yielding  $E = 5.44 \pm 0.03$  keV, flux  $n = 5.03_{-2.01}^{+2.02} \times 10^{-6}$  photons  $\text{cm}^{-2}\text{s}^{-1}$  and equivalent width  $46 \pm 16$  eV. Addition of a second line of the same width yielded a further improvement  $\Delta\chi^2 = 34$ ,  $E = 5.95 \pm 0.05$  keV, line flux  $n = 5.05_{-1.95}^{+2.05} \times 10^{-6}$  photons  $\text{cm}^{-2}\text{s}^{-1}$ , with an equivalent width of  $44_{-16}^{+17}$  eV and a final fit statistic  $\chi^2 = 117/97$  *d.o.f.* In this fit the flux and equivalent width of the Fe K $\alpha$  line were  $n = 1.59 \pm 0.23 \times 10^{-5}$  and  $195 \pm 24$  eV respectively.

To further examine the source behavior at low flux levels we isolated the lowest flux subset of the 2005 data using an intensity filter based upon the 0.5-10 keV band count rate, taking data below a threshold of 0.47 ct  $\text{s}^{-1}$  (per FI XIS). The intensity

cut effectively removed the periods of source flaring from consideration. This filtering thus resulted in a very-low-state spectrum that had a mean 2–10 keV flux  $6.1 \times 10^{-12}$  erg  $\text{cm}^{-2}\text{s}^{-1}$ . Again, fitting a simple absorbed continuum model over 3–10 keV leaves two strong positive residual features between 5–6 keV (Figure 4) confirming the prominence of the 5.44 keV line at low flux levels and indicating the possible presence of emission at 5.95 keV.

### 3.4. The Full Model

To assess the full properties of the source and investigate the robustness of the line detections to the continuum model used, we then fit over 0.75-50 keV (the full band of the *Suzaku* data). We simultaneously fit spectra from the three *Suzaku* observations. The 2008 HETG exposure (that overlapped the 2008 Nov 6 *Suzaku* observation) shows a wealth of absorption and emission lines that can be modeled using three zones of ionized gas (Lobban et al. 2010); those soft-band absorbers were fixed in the *Suzaku* fit, after which two additional gas layers were required to accurately model the source across the full *Suzaku* bandpass. The fit also included an Fe K $\alpha$  emission line fixed at a width of  $\sigma = 50$  eV as before. Finally, an absorbed ionized reflector was included to account for the curvature in the soft band. The full model is detailed in Table 2 and the fit is illustrated in Figure 5. The marked spectral variability observed (Figure 5) can be accounted for by allowing variations in the covering fraction of one absorbing layer (having  $N_H \sim 10^{23}$   $\text{cm}^{-2}$ ,  $\log \xi \sim 0.18$ ), a solution that is similar to other well-studied AGN of this class (e.g. Pounds et al. 2004; Risaliti et al. 2007; Miller et al. 2008; Turner et al. 2008). This fit yielded  $\chi^2 = 947/547$  *d.o.f.* with the overall curvature modeled well across all epochs and the residual  $\chi^2$  contributed mainly by some unmodeled spectral features. The addition of a line ( $\sigma = 50$  eV) constrained to lie in the range 3 - 8 keV yielded a detection at  $5.44 \pm 0.03$  keV and improved the fit statistic by  $\Delta\chi^2 = 20$ ; addition of another line under the same constraints gave  $5.98 \pm 0.05$  keV and  $\Delta\chi^2 = 9$  improvement to the fit. We conclude that the high significance for the detection of the 5.44 keV line is robust to the continuum used while the significance of the detection of a line at 5.95 keV

is sensitive to the continuum form assumed.

### 3.5. A Critical Examination of the Reality of the Lines

Before proceeding any further with the modeling, we performed several checks to be assured that the new line is attributable to the AGN and is significant. First, to confirm that the line is not an artifact of poor background subtraction, we examined the background spectrum and calibration source data. First we note that the background comprises just 2.5% of the total count rate in the 5-7 keV band for the XIS spectral data when the source is at its lowest flux level, during 2005 and 1.3% when the source is brighter, during 2008. Regarding the line at 5.44 keV, we found there to be no line emission evident at that energy in the background spectrum. Fitting the background spectra from the three *Suzaku* observations we obtained an upper limit (90% confidence) for the flux of a line at 5.44 keV in the background spectrum  $n < 4.14 \times 10^{-8}$  photons  $\text{cm}^{-2}\text{s}^{-1}$ , i.e. < 1% of the detected line flux.

The lack of a feature at comparable flux or equivalent width in the background data also rules out an origin of the 5.44 keV line as a detector feature. We then examined each XIS independently, and found the 5.44 keV line to be significantly detected in each XIS unit independently, further verifying the reality of the reported feature (Figure 6).

Regarding the more tentative line at 5.95 keV: the XIS chip does include a Mn calibration source emitting a line at 5.9 keV for the purpose of calibration of the XIS energy scale. The calibration source is located at the chip edge and the counts from that source are obviously conservatively excluded from any source and background extraction cells for scientific analysis. However, we do detect a weak Mn  $K\alpha$  emission in the background spectrum. The Mn contamination is at a level < 10% of the measured line strength in the AGN spectrum. As the source extraction cell is further from the Mn calibration source than the background cell and therefore subject to less contamination, we estimate the Mn line contamination from the calibration source to be < 10% for the 2005 spectrum. In spectral fitting, the greatest concern for the Mn line is the possible contamination by the weak broadened Fe  $K\alpha$  emission evident in the

fit to eigenvector 1 (Miller et al. 2009) which may lead to the strength of the Mn line being overestimated from simple fits. Because of the various issues associated with a clean measurement of any line at 5.95 keV and the sensitivity to the continuum form assumed we concentrate only on the strong line detection at 5.44 keV.

To confirm the significance of the line we performed Monte Carlo simulations using the method described in Porquet et al. (2004) and in Markowitz et al. (2006). We took the null hypothesis to be that the spectrum is simply an absorbed power-law continuum with parameters derived from fitting the broad-band data but allowing for the statistical uncertainty on the continuum parameters and including the narrow Fe  $K\alpha$  line whose presence is well-established in this source (Lobban et al. 2010). We used the XSPEC command *fakeit* to create 3000 fake *Suzaku* spectra with photon statistics expected from the 2005 exposure, assuming the same instruments to be operational as for the actual observation. The simulated data were grouped to the HWHM energy-resolution of the instruments, the same as the observational data. Following the procedure used to test the real data for the presence of a narrow line, we fitted each fake spectrum to obtain the values of  $\Delta\chi^2$  obtained from statistical fluctuations in the data. To map the distribution of  $\Delta\chi^2$  across the simulated spectra, each simulated spectrum was fitted over the 3-10 keV energy range, stepping through using energy bins whose centers were increased in increments of 100 eV. The line energy was allowed to be free within each energy bin tested and the value of  $\Delta\chi^2$  was recorded at each point in the spectrum. This method makes no assumptions about the energy at which a line might be detected and over the course of the testing, all energies are tested for the presence of a line. When we fit the simulated data we are testing whether we can produce, from statistical fluctuations, a contribution to  $\chi^2$  at the same or greater level as found in the actual data at any energy in the range of interest. The fits to the simulated data yield a distribution of  $\Delta\chi^2$  for comparison with the actual data. We found the most extreme statistical fluctuation to yield a  $\Delta\chi^2$  contribution of 19.3 in the 3-10 keV band in the set of simulated data (i.e. in 3000 simulations no false line appears at any energy contributing  $\Delta\chi^2 = 32$  as found in

2005 data). Thus the probability of satisfying the null hypothesis is  $p < 3.3 \times 10^{-4}$  for the line found at 5.44 keV.

### 3.6. Application of a Disk Hotspot Model

As an alternative to modeling using individual Gaussian lines, we fitted the data using a single disk line from a narrow annulus, such that the red horn of such a line might explain the peak at 5.44 keV. We assumed the system to contain a non-rotating black hole, that the line is Fe  $K\alpha$  emission from neutral material (at 6.4 keV), that the emissivity pattern across the disk can be described by  $r^{-q}$  where the emissivity index  $q = -2.5$  and that the hotspot exists over a narrow annulus of width  $\Delta r = 1r_g$ . We used the same baseline model as for testing the Gaussian lines (section 3.3).

To fit the 5.44 keV peak as the red Doppler horn of a disk-line requires an emitting radius  $21 \pm 3r_g$  (where  $r_g = GM_{BH}/c^2$  denotes gravitational radii) in a low inclination system with  $27_{-3}^{+1^\circ}$  with  $\chi^2 = 128/95 d.o.f.$ ; the corresponding blue horn is then predicted to lie at 6.62 keV and the data are consistent with that model. While there is evidence for line emission in the 6.5-7 keV regime, such lines are commonly observed as emission from ionized species of Fe, and thus the identification of emission blue-ward of 6.4 keV is currently ambiguous.

### 3.7. Examination of the Line Variability

Fits to the mean spectra from each observation have shown consistent line fluxes for Fe  $K\alpha$  and the line at 5.44 keV and these show an equivalent width that appears to have changed as the source flux varied. Figure 7 shows the ratio of data in the Fe  $K\alpha$  regime to a common local continuum fit; the fact that the source spectrum is steeper at high flux is reflected in the systematics of the residuals. To confirm the significance of the change in equivalent width we fit the 2008 data with a model that fixed the line equivalent width for the feature at 5.44 keV to that found during 2005; after refitting this resulted in a worse fit with  $\Delta\chi^2 = 142$ . Alternatively, fixing the flux of the new lines at the 2005 values and refitting, we found  $\Delta\chi^2 = 0$ , indicating that the line fluxes may be consistent with lines of constant flux across the data.

As the limits on line flux provide the potential

to distinguish between models, we tested all available high-quality data in a self-consistent manner. Taking the model from section 3.3 we fixed the line energy and width to specifically test the constancy of the 5.44 keV line. In addition to testing the mean spectrum from each *Suzaku* observation, we sub-divided the 2005 and 2008 exposures to sample the line more finely in flux. For 2005 an intensity selection was made on the 0.5-10 keV count rate at 0.47 ct s<sup>-1</sup> per XIS as before. For 2008 intensity selections were made  $< 2.0$  ct s<sup>-1</sup>/XIS (*i1*),  $2.0 - 3.0$  ct s<sup>-1</sup>/XIS (*i2*) and  $> 3.0$  ct s<sup>-1</sup>/XIS (*i3*). The results are shown in Table 3 where both the mean fits for each observation are tabulated, as well as the intensity-selected results. As noted previously, the line is required at a high level of confidence in the 2008 Nov 6 data (which is more sensitive to the features than the Nov 23 data, owing to the long exposure and high flux state of the source).

Table 3 shows line flux along with improvements in the fit-statistic and equivalent width for each fit. Note that the mean observation fits in Table 3 show slightly tighter constraints in line flux for 2005 compared to the values noted in section 3.3 because the initial fits to 2005 data had the line energy left free. The data are consistent with the 5.44 keV line existing at the same flux level throughout the *Suzaku* observations considered in Table 3 and the high significance of the line detection across several time slices of data provides compelling evidence for the reality of the line; conclusively ruling out the possibility of the line detection being a statistical fluctuation in the spectral data. Considering the three independent *Suzaku* detections of the line, as shown in Table 3 *Suzaku* observations 1,2 and 3 yield improvements to the fit  $\Delta\chi^2 = 32, 19, 19$  respectively and a probability of all three detections being false is  $p < 3 \times 10^{-11}$ .

We repeated the fits with the line energy allowed to be free and found the fitted energy to be consistent with 5.44 keV and that the line flux had not been significantly affected by freezing the energy.

To extend the test for line flux variations we reduced and fit the *XMM-Newton* spectra obtained during 2001 and 2002. We followed the standard reduction method for the pn data, as detailed by Ponti et al. (2006) and found the data to be consistent with the presence of a line at the same flux

as found using *Suzaku*. An independent analysis of the *XMM* data by de Marco et al. (2009) reported the presence of an excess of counts in the 5.4-6.2 keV band for NGC 4051, compared to their parameterization of the local continuum. Examination of the *XMM* data shows an excess of emission at  $\sim 6$  keV in the *XMM* spectra and so tentatively supports the possibility of that additional energy-shifted line in this source.

*BeppoSax* also observed NGC 4051, finding the source to be in a very low flux state during 1998 as reported by Guainazzi et al. (1998). We extracted and fit the archived *BeppoSax* Medium Energy Concentrator spectrum from units 2 and 3 (combined) and tested for the presence of the line. However, the data did not yield a significant detection of and the upper limits on line flux were very loose  $\sim 4 \times 10^{-5}$  photons  $\text{cm}^{-2}\text{s}^{-1}$  for a line at 5.44 keV. Given the poor constraint obtained we do not consider those data any further.

Combining the results from *Suzaku* and *XMM* observations (specifically, Table 3 lines 1,2,4,5,7-9 & 10) and comparing the data to a constant model yields  $\chi^2 = 4.7/7 \text{ d.o.f.}$  Further to this test, we split the data by time instead of intensity and repeated the test, reaching the same conclusion, i.e. that the data are consistent with a line of constant flux over a timescale of several years and over large changes in observed continuum flux. The limits on measured line fluxes mean we can rule out line variability greater than a factor  $\sim 2$  in the line flux sampled on these timescales, across the baseline time period considered.

#### 4. Discussion

While numerous claims exist in the literature for emission lines at unexpected energies (see Turner & Miller 2009a, for a review), the reality of the lines has been questioned by some. Vaughan & Uttley (2008) considered 38 published results on transient emission and absorption lines reported in the literature: those authors find a linear relationship between the fitted feature strength and its uncertainty. Vaughan & Uttley (2008) noted that observations with more signal apparently reveal weak lines but do not show tightly constrained strong lines which should sometimes also show up by chance. The conclusion of the Vaughan & Uttley (2008) literature review

was that there is a publication bias in reporting of these results, and that many of the reported detections are merely statistical fluctuations. This question has now been addressed with two systematic analyses of samples of AGN. Tombesi et al. (2010) present a study of the occurrence and reality of energy-shifted absorption lines in a sample of AGN finding a deviation from the linear relationship of line equivalent width (EW) and uncertainty found by Vaughan & Uttley (2008) in the sense that their distribution showed more significant detections of lines in sources studied. Tombesi et al. (2010) compare their absorption line measurements with those of the Fe  $K\alpha$  emission in the same sources and show that these two sets of measurements follow the same distribution in the EW/uncertainty plane. Tombesi et al. (2010) conclude that the absorption line detections are generally not statistical fluctuations and that the absence of well-constrained detections of strong features in the Vaughan & Uttley (2008) analysis may be due in part to a limit on the ability of current X-ray instruments to detect such lines. It also would appear likely that long observations of bright sources may not have been proposed or approved early in the *XMM* and *Suzaku* missions and so the sample of observations completed to date is likely biased against those that would have shown tightly constrained energy-shifted lines: such a bias may explain at least some of the effect discussed by Vaughan & Uttley (2008). Another recent study by de Marco et al. (2009) undertook a systematic analysis of a sample of bright Seyfert 1 galaxies and confirmed many of the individual detections of energy-shifted emission lines claimed in the literature, supporting the general reality of the phenomenon by consideration of the statistics of the sample results as a whole. With conflicting views in the literature it is clear that the detection of significant new examples of the energy-shifted line phenomenon is very important at this time.

##### 4.1. Hard X-ray Line Emission in NGC 4051

NGC 4051 can be modeled using a powerlaw continuum covered by multiple zones of gas, several in the column density range  $10^{23} - 10^{24} \text{ cm}^{-2}$ , that impart emission and absorption features to the X-ray spectrum. The marked spectral vari-



ability with observed flux can be explained by changes in covering of the powerlaw continuum by one of the high-column absorbers, as found for other similar AGN (e.g. Pounds et al. 2004; Risaliti et al. 2007; Miller et al. 2008; Turner et al. 2008). Significant line emission has been observed at 5.44 keV in the 2005 *Suzaku* observation of NGC 4051. Comparison of low and high-state X-ray data for NGC 4051 shows that the newly-discovered line appears prominent in the low-flux state along with the narrow component of Fe K $\alpha$  emission from neutral gas, as expected if the observed low state is simply those times when a relatively large fraction of the continuum is suppressed by absorption.

The most recent measurements indicate NGC 4051 to have a black hole mass  $M_{BH} = 1.73^{+0.55}_{-0.52} \times 10^6 M_{\odot}$  and a radius for the  $H\beta$  broad line region (BLR)  $R_{BLR} = 1.87^{+0.54}_{-0.50}$  light days (Denney et al. 2009). The  $H\beta$  FWHM in the rms spectrum of Denney et al. is  $1034 \pm 41 \text{ km s}^{-1}$  (although those authors used the velocity dispersion rather than the FWHM in their mass estimate). If we assume the same geometrical correction factor between line width and circular velocity as those authors to scale the respective FWHM measurements, the line width of Fe K $\alpha$  is indicative of an origin at  $r \simeq 1.87(1034/5540)^2 \simeq 0.065$  light days, or  $2 \times 10^{14} \text{ cm}$ , with a 90 percent confidence range  $8.6 \times 10^{13} - 1.7 \times 10^{15} \text{ cm}$ . As we have scaled to the optical reverberation results, this radius estimate is secure provided the X-ray and optical line-emitting regions have similar structure and orientation with respect to the observer, but the large uncertainty is dominated by the uncertainty in the line width measurement. Further to the measurement error is the uncertainty as to whether, as suggested by the form of eigenvector 1, the Fe K $\alpha$  emission has both broad and narrow components, in which case we would have to conclude that we are seeing contributions from regions both within and outside of the region noted above. Given the limited signal-to-noise in the regime of Fe K $\alpha$  in the HEG data this question remains open with current data.

In the single component model for Fe K $\alpha$  emission, spectral fitting to the HEG plus *Suzaku* data yields an Fe K $\alpha$  emission line of flux  $n = 1.90 \pm 0.40 \times 10^{-5} \text{ photons cm}^{-2} \text{ s}^{-1}$ . The strength of the Fe K $\alpha$  line emission, normalized to the illu-

minating continuum, can be used to set limits on the reprocessing gas in which it arises. Following Yaqoob et al. (2010) and correcting for the continuum slope found here, we estimate an efficiency for the production of line photons (defined as the ratio of line flux to incident flux above the ionization edge) to be  $x_{\text{FeK}\alpha} \sim 0.018$ . The line measured here sets a lower limit on the column density of the emitting region  $N_H > 10^{24} \text{ cm}^{-2}$  and in the toroidal reprocessor model suggests a global covering factor  $\sim 0.9$  with an approximately face-on view down the pole of the structure. As it is difficult to determine the intrinsic continuum strength from the observed continuum the interpretation of these data in the context of the toroidal model is subject to some uncertainty that in turn, leaves the derived global covering factor uncertain by a factor of a few.

Combining the minimum column density of the line-of-sight gas with the radial constraints and knowledge of the gas having a high covering fraction yields a mass estimate  $\gtrsim 4 \times 10^{-4} M_{\odot}$  for the gas emitting the Fe K $\alpha$  line, assuming the nominal radius of emission of  $2 \times 10^{14} \text{ cm}$ . The 90 percent confidence uncertainty in the distance translates into a confidence region on the mass lower limit of  $5 \times 10^{-5} - 0.1 M_{\odot}$ . If a torus is not the true geometry of the gas then, of course, the covering factor could be different to this value. Further to the uncertainties mentioned, the line may be comprised of contributions from two regions. Taking instead the two-component fit to the Fe K $\alpha$  profile then the column and/or global covering requirements are reduced for each of the two emitting regions.

The PCA decomposition (Miller et al. 2009) suggests a link between the origin of the Fe K $\alpha$  line and that of the line at 5.44 keV. Observation of similar lines in other AGN has motivated discussion of several possible origins, including spallation and hotspot emission from the accretion disk.

The solution found in the context of the disk hotspot model suggests that the emitting radius is between  $18 - 24 r_g$ . The orbital timescales at these radii are  $\sim 4 - 6 \text{ ks}$  for  $18-24 r_g$  for the black hole mass considered here. The observation of a steady line flux over 2005 - 2008 provides a constraint on the disk hotspot hypothesis as the three year baseline is equivalent to  $\sim 16,000 - 24,000$

orbits about the black hole over the radial range of interest (and tens of orbits just considering the line persistence within the 2005 observation). Theoretical modeling indicates that hotspot events are not expected to last longer than a few orbital timescales at these small radii (Karas et al. 2001) and that a given hotspot would suffer measurable flux and energy changes as the material spirals in (Dovčiak et al. 2004). However, persistent steady lines could arise from a special radius in the disk or other rotating reprocessor without any constraining expectation of flux or energy variability. If the special radius is interpreted as the truncation radius of the inner disk this places the innermost edge of the disk at  $18\text{--}24r_g$ . The inner edge of the disk may emit more strongly than the rest of the structure if it is inflated due to radiation pressure as in the advection-dominated accretion flow scenario. Assuming the bolometric luminosity to be  $L_{bol} = 10^{43}\text{erg s}^{-1}$  (Vasudevan & Fabian 2009, corrected to the Tully-Fisher distance 15.2 Mpc, Russell 2004) and assuming a radiative efficiency  $\eta^{\text{BOL}} = 0.05$  the mass accretion rate is estimated to be  $\dot{M} \simeq 0.0035 M_{\odot}\text{year}^{-1}$ ,  $\sim 10\%$  of the Eddington accretion rate. For such high accretion rates the transition from thin disk to an advection-dominated accretion flow may occur anywhere up to a radius of  $\sim 2000r_g$  (Narayan et al. 1998) and so our fitted radius is consistent with such a scenario. If features on the truncated edge of the disk are steady in flux, as found for the line in NGC 4051, then Galactic binaries would also be expected to show such lines in the low flux state and the absence of such would disfavor the truncated disk origin for the lines. While similar lines have not been reported to date for Galactic black hole binaries (see Done et al. 2007, for a review), constraints on such lines have not yet been explored in that source class, leaving this an open question.

In an alternative model, the fact that the specific energy of the line is coincident with  $K\alpha$  emission from neutral Cr (5.4 keV) prompts a renewed interest in the spallation of Fe as a mechanism for enhancing otherwise weak lines, especially since PCA is consistent with a common origin for the new line and the neutral component of Fe. In a companion paper, Turner & Miller (2009b), explore in detail the spallation interpretation of the new result, extending the work of Skibo (1997) in

the light of new understanding about the environs of active nuclei. Turner & Miller (2009b) find the observed abundance enhancement to be high and that these extreme enhancement effects are most likely to be achieved in gas out of the plane of the accretion disk. In such a picture, the timescale for spallation may be as short as a few years if the cosmic ray output is comparable to the bolometric output of the nucleus. Turner & Miller (2009b) also estimate the expected radio and  $\gamma$ -ray flux from the proposed spallation process in NGC 4051 and find predictions to be consistent with current flux measurements in those bands.

## 5. Conclusions

Our analysis of *Suzaku* data from NGC 4051 taken during 2005 and 2008 has revealed line emission at 5.44 keV in the rest-frame of the galaxy. We have established the reality of the line at  $> 99.9\%$  confidence in data from 2005, supported by Monte Carlo simulations that show the probability of the line being a statistical fluctuation is  $p < 3.3 \times 10^{-4}$ . The possibility of the line arising from a statistical fluctuation in the spectral data has been firmly ruled out by establishing its detection in time-sliced data. Further to this, we have confirmed the line to be evident in all three XIS units independently, and established that the observed line is inconsistent with arising from the X-ray background.

The source spectrum varies with flux, and the low state is dominated by a hard spectral form with the new line plus the neutral component of Fe  $K\alpha$  emission superimposed upon that, suggestive of a common origin for both. The line has an equivalent width during 2005 of about 45 eV while the Fe  $K\alpha$  line is measured at 195 eV. These reprocessed signatures show up prominently in the source low state when the continuum is suppressed by the highest covering fraction of absorption.

As disk hotspot emission would be expected to vary in flux and energy over relatively short timescales, the limits on line variability disfavor this particular origin although the data remain consistent with emission from a special location such as the innermost radius of the accretion disk. The alternative picture, that the line is Cr I  $K\alpha$  emission following spallation of Fe is also found to be a good explanation of the data: that possibility

and its implications are explored in a companion paper.

TJT acknowledges NASA grant NNX08AL50G. LM acknowledges STFC grant number PP/E001114/1. We are grateful to the anonymous referee whose comments significantly improved this manuscript: we also thank the *Suzaku* operations team for performing this observation and providing software and calibration for the data analysis. This research has also made use of data obtained from the High Energy Astrophysics Science Archive Research Center (HEASARC), provided by NASA's Goddard Space Flight Center.

## REFERENCES

- Boldt, E. & Leiter, D. 1987, ApJ, 322, L1
- Collinge, M. J., Brandt, W. N., Kaspi, S., Crenshaw, D. M., Elvis, M., Kraemer, S. B., Reynolds, C. S., Sambruna, R. M., & Wills, B. J. 2001, ApJ, 557, 2
- de Marco, B., Iwasawa, K., Cappi, M., Dadina, M., Tombesi, F., Ponti, G., Celotti, A., & Miniutti, G. 2009, A&A, 507, 159
- Denney, et.al. 2009, arXiv:0904.0251
- Done, C., Gierliński, M., & Kubota, A. 2007, A&A Rev., 15, 1
- Dovčiak, M., Bianchi, S., Guainazzi, M., Karas, V., & Matt, G. 2004, MNRAS, 350, 745
- Fukazawa, et al. 2009, PASJ, 61, 17
- Gruber, D. E., Matteson, J. L., Peterson, L. E., & Jung, G. V. 1999, ApJ, 520, 124
- Guainazzi, et.al. 1998, MNRAS, 301, L1
- Karas, V., Martocchia, A., & Subr, L. 2001, PASJ, 53, 189
- Koyama, et.al. 2007, PASJ, 59, 23
- Leahy, D. A. & Creighton, J. 1993, MNRAS, 263, 314
- Lobban, A., Reeves, J., Turner, T. J., Miller, L., Braitto, V., Crenshaw, D., & Kraemer, S. 2010, in preparation
- Markowitz, A., Reeves, J. N., & Braitto, V. 2006, ApJ, 646, 783
- Miller, L., Turner, T. J., Reeves, J. N., George, I. M., Kraemer, S. B., & Wingert, B. 2007, A&A, 463, 131
- Miller, L., Turner, T. J., & Reeves, J. N. 2008, A&A, 483, 437
- Miller, L., Turner, T. J., Reeves, J. N., Lobban, A., Kraemer, S. B., & Crenshaw, D. M. 2009, arXiv:0912.0456
- Mitsuda, et.al. 2007, PASJ, 59, 1
- Narayan, R., Mahadevan, R., & Quataert, E. 1998, in Theory of Black Hole Accretion Disks, ed. M. A. Abramowicz, G. Björnsson, & J. E. Pringle, 148
- Palmeri, P., Mendoza, C., Kallman, T. R., Bautista, M. A., & Meléndez, M. 2003, A&A, 410, 359
- Ponti, G., Miniutti, G., Cappi, M., Maraschi, L., Fabian, A. C., & Iwasawa, K. 2006, MNRAS, 368, 903
- Porquet, D., Reeves, J. N., Uttley, P., & Turner, T. J. 2004, A&A, 427, 101
- Pounds, K. A., Reeves, J. N., King, A. R., & Page, K. L. 2004, MNRAS, 350, 10
- Risaliti, G., Elvis, M., Fabbiano, G., Baldi, A., Zezas, A., & Salvati, M. 2007, ApJ, 659, L111
- Russell, D. G. 2004, ApJ, 607, 241
- Skibo, J. G. 1997, ApJ, 478, 522
- Steenbrugge, K. C., Fenovčík, M., Kaastra, J. S., Costantini, E., & Verbunt, F. 2009, A&A, 496, 107
- Takahashi, et.al. 2007, PASJ, 59, 35
- Terashima, et.al. 2009, PASJ, 61, 299
- Tombesi, F., Cappi, M., Reeves, J. N., Palumbo, G. G., Yaqoob, T., Braitto, V., & Dadina, M. 2010, submitted to ApJ
- Turner, T. J., Kraemer, S. B., & Reeves, J. N. 2004, ApJ, 603, 62

- Turner, T. J. & Miller, L. 2009a, *A&A Rev.*, 17, 47
- Turner, T. J. & Miller, L. 2009b, arXiv:0912.3479
- Turner, T. J., Mushotzky, R. F., Yaqoob, T., George, I. M., Snowden, S. L., Netzer, H., Kraemer, S. B., Nandra, K., & Chelouche, D. 2002, *ApJ*, 574, L123
- Turner, T. J., Reeves, J. N., Kraemer, S. B., & Miller, L. 2008, *A&A*, 483, 161
- Vasudevan, R. V. & Fabian, A. C. 2009, *MNRAS*, 392, 1124
- Vaughan, S. & Uttley, P. 2008, *MNRAS*, 390, 421
- Yaqoob, T., George, I. M., Kallman, T. R., Padmanabhan, U., Weaver, K. A., & Turner, T. J. 2003, *ApJ*, 596, 85
- Yaqoob, T., Murphy, K. D., Miller, L., & Turner, T. J. 2010, *MNRAS*, 401, 411

Table 1: The Observation Log

Observation	Date	ct s <sup>-1</sup>	Flux <sup>1</sup>	Exposure time
<i>XMM 1</i>	2001-05-16	19.27	2.31	39.6
<i>XMM 2</i>	2002-11-22	3.15	0.56	150.9
<i>Suzaku 1</i>	2005-11-10	0.45	0.87	120
<i>Suzaku 1-i1</i>	2005-11-10	0.32	0.70	80.0
<i>Suzaku 1-i2</i>	2005-11-10	0.71	1.26	39.6
<i>Suzaku 2</i>	2008-11-06	2.06	2.42	275
<i>Suzaku 2-i1</i>	2008-11-06	1.37	1.76	129.2
<i>Suzaku 2-i2</i>	2008-11-06	2.38	2.75	92.9
<i>Suzaku 2-i3</i>	2008-11-06	3.63	3.89	40.6
<i>Suzaku 3</i>	2008-11-23	1.42	1.79	78

*i1*, *i2* etc refer to the intensity selected data, see text for details

<sup>1</sup>The observed 2-10 keV flux in units 10<sup>-11</sup>ergs cm<sup>-2</sup> s<sup>-1</sup>

<sup>2</sup>Mean exposure time in the CCD instruments in ks

<sup>3</sup>Mean count rate in the 0.5-10 keV band given per FI XIS in the case of *Suzaku* or for the pn in the case of *XMM*

Table 2: The Spectral Model

Parameter	2005	2008a	2008b
$\Gamma$	2.47±0.02	<i>l</i>	<i>l</i>
$PL_{norm}^1$	0.58 ± 0.01	1.818 ± 0.004	1.283 ± 0.005
$N_{H4}^2$	2.17 ± 0.23 <sup>2</sup>	<i>l</i>	<i>l</i>
Log $\xi_4^3$	3.40±0.01	<i>l</i>	<i>l</i>
$N_{H5}^2$	1.17±0.04	<i>l</i>	<i>l</i>
Log $\xi_5$	0.18 <sup>+0.15</sup> <sub>-0.16</sub>	<i>l</i>	<i>l</i>
<i>Covering</i> ( $N_{H5}$ )	71±2%	35 ± 2 %	38 ± 2%
$Pex_{qbund}^4$	0.40±0.03	<i>l</i>	<i>l</i>
$Pex_{norm}^4$	3.84 ± 0.19	5.41 ± 0.26	4.84 ± 0.28
$N_{H6}^1$	50.0 <sup>p</sup> <sub>-5.0</sub>	<i>l</i>	<i>l</i>
Log $\xi_6$	2.62±0.05	<i>l</i>	<i>l</i>
Log <i>Reflion</i> $\xi$	2.94 ± 0.07	<i>l</i>	<i>l</i>
<i>Reflion</i> $_{norm}$	1.03 × 10 <sup>-7</sup>	<i>l</i>	<i>l</i>

<sup>1</sup> PL normalization in units 10<sup>-2</sup>photon cm<sup>-2</sup>s<sup>-1</sup> at 1 keV

<sup>2</sup> Column densities in units of 10<sup>23</sup>cm<sup>-2</sup>

<sup>3</sup> This zone is outflowing at  $\sim$  5500 km/s -see Lobban et al. 2010 and also Collinge et al. 2001; Steenbrugge et al. 2009

<sup>4</sup> Parameters of the pexrav component, abundance as fraction of solar and normalization in units 10<sup>-2</sup>photon cm<sup>-2</sup>s<sup>-1</sup> at 1 keV;

Normalizations are in photons cm<sup>-2</sup> s<sup>-1</sup>

*l* indicates a parameter that was linked to be the same for all epochs

All components are also fully covered by the Galactic column of neutral gas with  $N_H(Gal) = 1.3 \times 10^{20}$ cm<sup>-3</sup> plus three zones of ionized gas determined from HETG feature measurements (Lobban et al. 2010) and thus frozen in this fit.  $N_{H1} = 9.6 \times 10^{19}$ cm<sup>-2</sup>, log  $\xi_1 = 0.90$ ;  $N_{H2} = 5.12 \times 10^{20}$ cm<sup>-2</sup>, log  $\xi_2 = 2.08$ ;  $N_{H3} = 1.08 \times 10^{21}$ cm<sup>-2</sup>, log  $\xi_3 = 2.14$

$N_{H5}$  covers a fraction of the powerlaw (only)

$N_{H6}$  covers the ionized reflector (only)

Table 3: X-ray Line Emission in the 3-10 keV band

Observation	$F_{6.40}^1$	$EW_{6.40}$	$\Delta\chi_{6.40}^2$	$F_{5.44}^1$	$EW_{5.44}$	$\Delta\chi_{5.44}^2$	$\chi^2/d.o.f.^2$
<i>XMM 1</i>	$23.79^{+3.28}_{-3.30}$	$95^{+15}_{-15}$	143	$0.86^{+3.24}_{-0.86}$	$23^{+87}_{-23}$	0	117/109
<i>XMM 2</i>	$18.07^{+2.58}_{-2.16}$	$205^{+16}_{-16}$	158	$2.50^{+1.91}_{-2.09}$	$37^{+30}_{-30}$	3	146/108
<i>Suzaku 1</i>	$19.05^{+1.60}_{-1.60}$	$155^{+24}_{-24}$	379	$5.03^{+1.44}_{-1.45}$	$46^{+16}_{-16}$	32	150/100
<i>Suzaku 1-i1</i>	$18.30^{+1.86}_{-1.87}$	$201^{+20}_{-21}$	261	$5.18^{+1.59}_{-1.60}$	$46^{+14}_{-14}$	27	107/100
<i>Suzaku 1-i2</i>	$20.99^{+3.06}_{-3.07}$	$149^{+22}_{-22}$	127	$4.84^{+2.87}_{-2.87}$	$26^{+15}_{-15}$	8	136/100
<i>Suzaku 2</i>	$22.31^{+1.65}_{-1.65}$	$91^{+7}_{-7}$	160	$4.23^{+1.57}_{-1.57}$	$13^{+5}_{-5}$	19	182/100
<i>Suzaku 2-i1</i>	$21.95^{+2.02}_{-2.02}$	$120^{+11}_{-11}$	269	$2.35^{+1.99}_{-2.00}$	$10^{+8}_{-8}$	4	135/100
<i>Suzaku 2-i2</i>	$20.52^{+2.95}_{-2.95}$	$74^{+11}_{-11}$	131	$5.81^{+2.88}_{-2.88}$	$16^{+8}_{-8}$	11	117/100
<i>Suzaku 2-i3</i>	$27.75^{+5.15}_{-5.15}$	$75^{+14}_{-14}$	79	$6.80^{+5.10}_{-5.10}$	$14^{+10}_{-10}$	5	114/100
<i>Suzaku 3</i>	$19.98^{+3.02}_{-3.19}$	$107^{+14}_{-14}$	142	$4.31^{+2.69}_{-3.05}$	$17^{+12}_{-12}$	19	120/100

*i1, i2* etc refer to the intensity selected data, see text for details

<sup>1</sup>Line normalization in units  $10^{-6}$  photons  $\text{cm}^{-2}\text{s}^{-1}$  for a line having width  $\sigma = 50$  eV

<sup>2</sup>Fit statistic including both of the lines

Line equivalent widths are measured against the total observed continuum

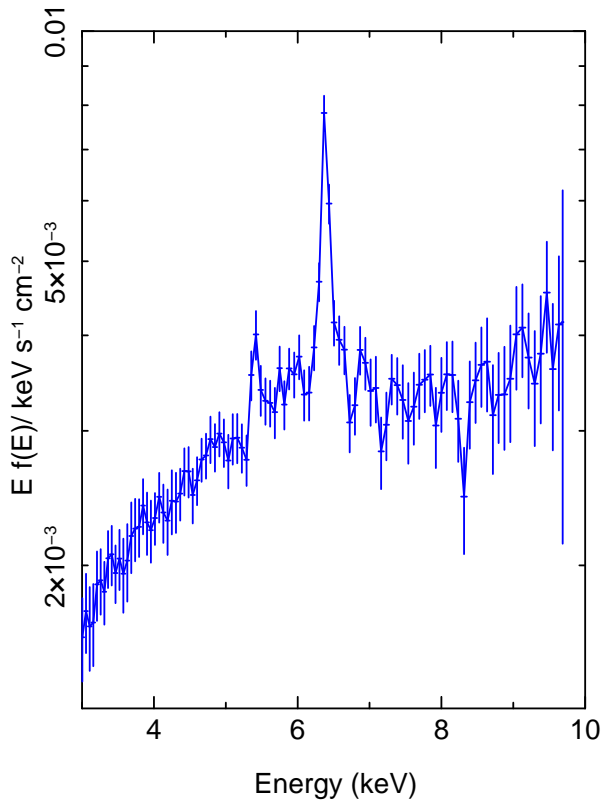


Fig. 1.— The offset component from the PCA decomposition of all of the 2005 and 2008 *Suzaku* XIS0 + 3 and PIN data. A strong narrow Fe  $K\alpha$  line is evident at 6.4 keV, along with emission at 5.4 and, more weakly, at 6 keV.

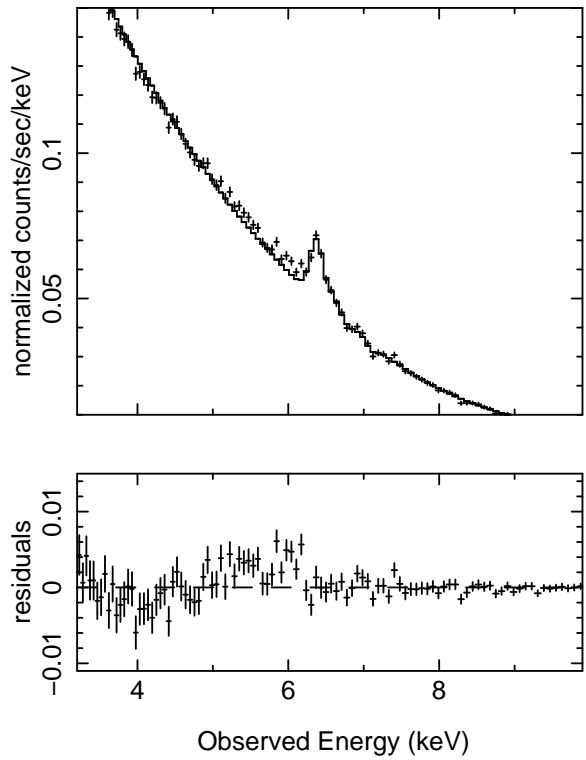


Fig. 2.— *Suzaku* XIS0 + 3 data and residuals from the mean 2008 Nov 6 spectrum, compared to an absorbed powerlaw plus Gaussian line at 6.4 keV

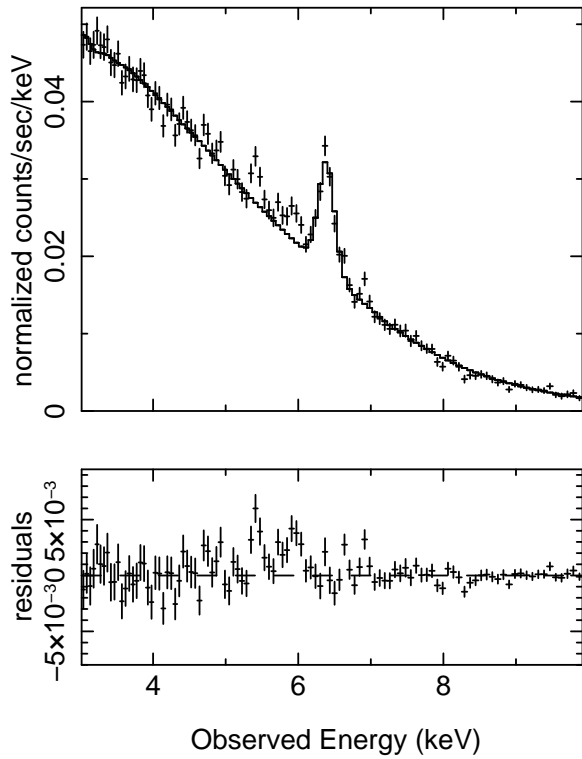


Fig. 3.— *Suzaku* XIS0 + 2 + 3 data and residuals from the mean 2005 spectrum, compared to an absorbed powerlaw plus Gaussian line at 6.4 keV, showing the residual excess counts at  $\sim 5.44$  and 5.95 keV

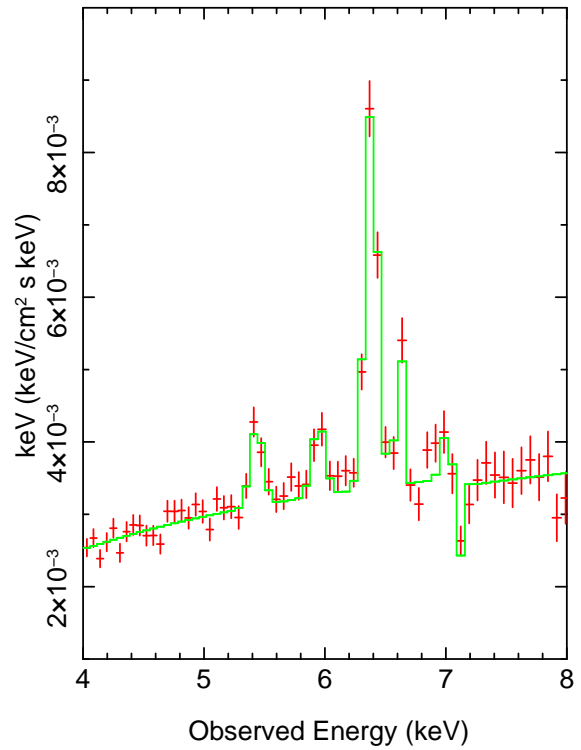


Fig. 4.— The very low state data (red crosses) from within the 2005 observation shown with the model line (solid green), illustrating the emission and absorption lines present in the data.



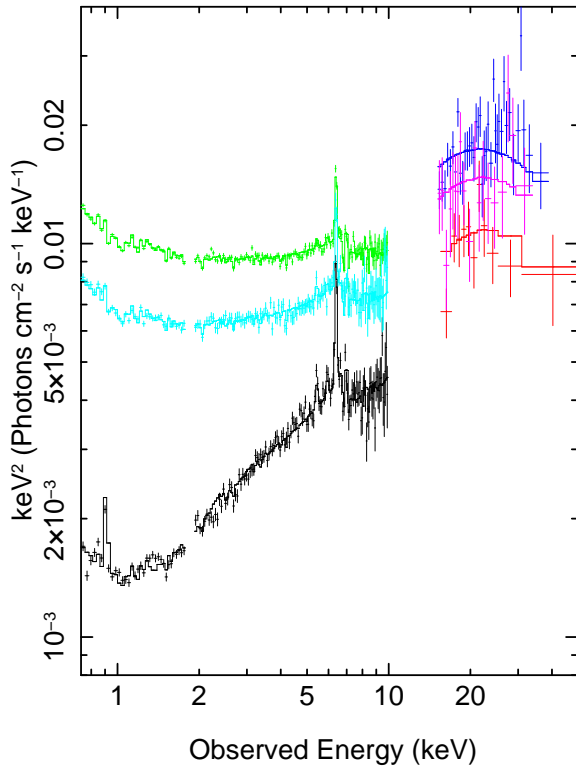


Fig. 5.— The 2005 (XIS is black, PIN is red), 2008 Nov 6 (XIS green, PIN ) and Nov 23 (XIS pale blue, PIN magenta) data along with the broad-band model described in the text.

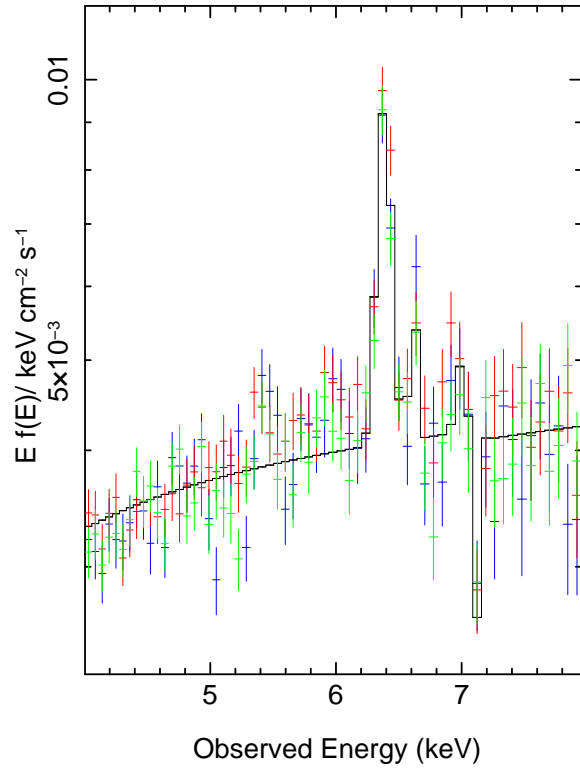


Fig. 6.— The 2005 data for the three XIS detectors against the continuum model (black line); blue is XIS0, red is XIS2 and green is XIS3

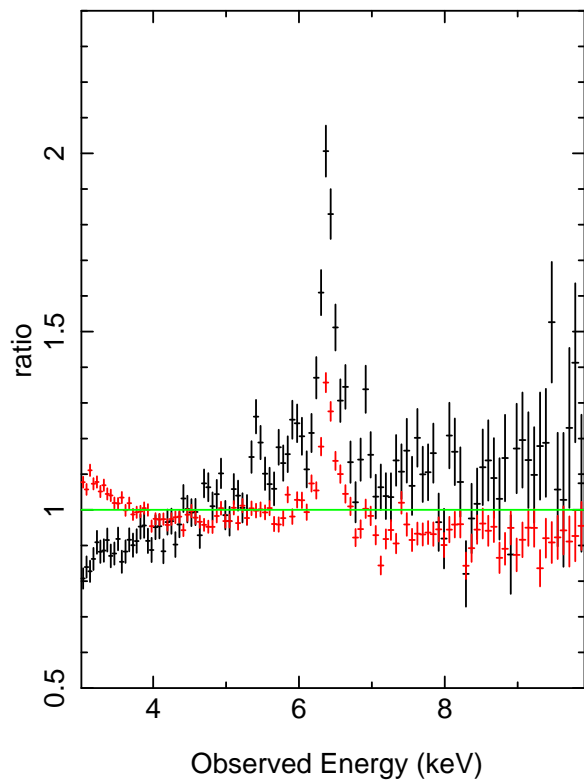


Fig. 7.— *Suzaku* data shown as a ratio to the mean local continuum model. The red line is the data from 2008 Nov 6 and the black line is the data from 2005.